**Ocean Science
Discussions**

Field measurements of aerosol production from whitecaps in the open ocean

**S. J. Norris[1], I. M. Brooks[1], B. I. Moat[2], M. J. Yelland[2], G. de Leeuw[3,4,5],
R. W. Pascal[2], and B. Brooks[1]**

[1]School of Earth and Environment, University of Leeds, UK
[2]National Centre of Oceanography, Southampton, UK
[3]Climate Change Unit, Finnish Meteorological Institute, Helsinki, Finland
[4]Department of Physics, University of Helsinki, Helsinki, Finland
[5]Netherlands Organisation for Applied Scientific Research TNO, Utrecht, The Netherlands

Correspondence to: S. J. Norris (snorris@env.leeds.ac.uk)

Title Page

Abstract	Introduction
Conclusions	References
Tables	Figures

◄◄	►►
◄	►
Back	Close

Full Screen / Esc

Printer-friendly Version

Interactive Discussion

Abstract

Simultaneous measurements of near-surface aerosol and bubble spectra were made during five buoy deployments in the open ocean of the North Atlantic and used to estimate aerosol fluxes per unit area of whitecap. The measurements were made during two cruises as part of the SEASAW project, a UK contribution to the international SO-LAS program. The mean bubble number concentrations for each deployment are in broad agreement with other open ocean spectra and are consistently one to two orders of magnitude lower than previous laboratory and surf zone studies. This suggests that the aerosol fluxes estimated above open ocean whitecaps will differ to those from over the surf zone and laboratory whitecaps due to the differences in the size and number of bursting bubbles. Production fluxes per unit area of whitecap are estimated from the mean aerosol concentration for each buoy deployment. They are found to increase with wind speed, and span the range of values found by previous laboratory and surf-zone studies for particles with radius at 80 % humidity, $R_{80} < 1\,\mu\text{m}$, but to drop off more rapidly with increasing size for larger particles. A possible cause of this difference in behavior is the significant difference in bubble spectra. Estimates of the mean sea spray flux were made by scaling the whitecap production fluxes with in-situ estimates of whitecap fraction. The sea spray fluxes are also compared with simultaneous individual eddy covariance flux estimates made during the cruise, and with a sea spray source function derived from them.

1   Introduction

Sea spray aerosol is an important component of the climate system and the largest single source of aerosol mass injected into the atmosphere after wind-blown dust (Hoppel et al., 2002). Under clear skies over the remote ocean sea salt aerosol is the dominant scatterer of incoming solar radiation (Haywood et al., 1999), it plays a significant role in controlling the microphysics and chemistry of marine stratocumulus (O'Dowd et

al., 1999), and provides a substantial sink for atmospheric trace gases, both natural and anthropogenic (O'Dowd et al., 2000). To quantify the effects of sea spray aerosol on the environment, a detailed knowledge of the numbers and sizes of aerosol particles produced at the ocean surface is required.

There are two production mechanisms for sea spray particles: mechanical tearing of water droplets (spume) from wave crests at high wind speeds, and the bursting of bubbles at the water surface. Bubbles form predominantly from breaking wind waves in the open ocean (Kolovayev, 1976); these entrain air into the near-surface water column producing a plume of bubbles (Blanchard and Woodcock, 1957), and as the bubble rise they form regions of foam at the surface – whitecaps. Other potential production mechanisms for bubbles include production by the respiration of phytoplankton (Medwin, 1970; Johnson and Wangersky, 1987), release from the sea bed (e.g. Leighton and Robb, 2008), gases coming out of solution as gas-saturated water warms (Norris et al., 2011), and where sea ice is present the release of bubbles trapped in melting ice or expelled during the freezing process (Wettlaufer, 1998).

Bursting bubbles produce droplets by two distinct mechanisms; disintegration of the bubble film produces a large number (100 s to 1000 s) of droplets smaller than about $R = 2\,\mu\text{m}$, while the collapse of the sides of the bubble cavity result in the ejection of a jet of water from the centre of the collapsing bubble which breaks into a handful of droplets of between about 1 and 50 µm radius. The precise size and number of droplets produced by a single bubble depends on the bubble size (Blanchard, 1983), water properties (Mårtensson et al., 2003) and the presence of surface active material (Morelli et al., 1974; Blanchard, 1990). The smallest bubbles produce only jet droplets, while the largest produce only film droplets; the limits between them are not well defined, however, and depend on the properties of both water and surface microlayer. Day (1964) found a bubble radius of $\sim 50\,\mu\text{m}$ to be the minimum size producing film droplets while Spiel (1997) found the limit to be 600 µm. The largest jet droplet produced by a bubble is roughly 1/10 the radius of the parent bubble (Blanchard, 1963; Spiel, 1994) with an

Field measurements of aerosol production

S. J. Norris et al.

Title Page

Abstract	Introduction
Conclusions	References
Tables	Figures

|◄| |►|

|◄| |►|

| Back | Close |

Full Screen / Esc

Printer-friendly Version

Interactive Discussion

upper limit on bubble radius for the production of jet droplets of approximately 3 mm (Spiel, 1997; Georgescu et al., 2002).

Turbulent air motion mixes the ejected droplets upwards, opposed by their gravitational fall speed, resulting in a change in particle spectra with altitude (Monahan, 1968; Wu et al., 1984; de Leeuw, 1989; Parameswaran, 2001). During transport, transformation due to coagulation, evaporation and chemical processes may occur, resulting in high variability in the aerosol's physical and chemical properties. Newly generated droplets shrink via evaporation until they reach a state of equilibrium with the ambient relative humidity. For ease of comparison aerosol spectra are usually adjusted to a reference humidity – commonly 80 %, with the radius denoted R_{80}. The size of a particle influences its life cycle in the atmosphere. Particles in the nucleation mode ($R_{80} < 0.1\,\mu\text{m}$) grow by condensation and coagulation, eventually becoming accumulation mode particles ($0.1 > R_{80} < 5\,\mu\text{m}$) which have the longest residence times. For particles with $R_{80} > 10\,\mu\text{m}$ an increasing fraction fall back to the surface before reaching equilibrium (Andreas et al., 2010), imposing an upper size limit on the resulting aerosol spectra. Turbulent mixing means that any measured aerosol spectrum will represent a mixture of newly generated with pre-existing aerosol.

Many parameterizations for the sea spray generation function have been proposed, based on a variety of observational techniques (See Lewis and Schwartz, 2004 for an overview). One approach has been to estimate the interfacial production flux from a unit area of whitecap and to scale this by the fractional area coverage of whitecaps on the sea surface, W, in turn often parameterized as a function of the mean local wind speed. It has usually been assumed that the production flux is independent of the nature and extent of the whitecap, including its production mechanism. One of the most commonly used such formulations is that of Monahan and O'Muircheartaigh (1986) which is based on the production flux of particles per unit area of whitecap obtained in a laboratory study (Spiel, 1983) and an empirical relationship for the whitecap fraction as a function of wind speed (Monahan and O'Muircheartaigh, 1980)

$$W = 3.84 \times 10^{-4} U_{10}^{3.41} \tag{1}$$

Title Page

Abstract | Introduction

Conclusions | References

Tables | Figures

|◄ | ►|

◄ | ►

Back | Close

Full Screen / Esc

Printer-friendly Version

Interactive Discussion

where U_{10} is the wind speed at 10 m above the sea surface, and W is in %. There are many different whitecap fraction parameterizations derived from photographs and videos of the sea surface from towers, aircraft, and ships. Anguelova and Webster (2006) provide an extensive summary of many studies, and find that they span a range of approximately 2–3 orders of magnitude at all wind speeds. It is generally recognized that whitecap fraction is zero for wind speeds less than about 3 m s^{-1} (Blanchard, 1963; Monahan, 1971).

The production flux of aerosol from a unit area of whitecap has been estimated from both laboratory studies (Monahan et al., 1982; Cipriano et al., 1983, 1987; Woolf et al., 1988; Mårtensson et al., 2003; Sellegri et al., 2006; Tyree et al., 2007; Keene et al., 2007; Facchini et al., 2008; and Fuentes et al., 2010) and measurements over natural whitecaps (Woodcock et al., 1963; Blanchard, 1969; de Leeuw et al., 2000; Clarke et al., 2006). The advantage of laboratory measurements is the ability to control the environmental conditions; however, it is difficult to create conditions truly representative of the open ocean, particularly those of well developed sea states, mixed seas or high winds. A more representative approach would be to make in situ estimates of the direct aerosol production from whitecaps at sea. However, making measurements in the open ocean close enough to the surface to isolate the aerosol generated by individual whitecaps from the background aerosol is difficult. Historically, optical particle counters have been heavy and physically bulky instruments, which are difficult to locate near the ocean surface. Therefore, the majority of the field measurements of sea spray particle number concentrations have been made between 5–25 m above the surface and then interpolated to a reference level for comparison (usually the surface or 10 m above mean surface level) (Andreas, 2002). New technology is now making small, lightweight, and relatively cheap sensors increasingly available (e.g. Hill et al., 2008) enabling measurements approaches that were not previously viable.

De Leeuw et al. (2000) and Clarke et al. (2006) used measurements over surf zone whitecaps to estimate the production of sea spray aerosol. Measuring over the surf zone allows the instruments to be located on solid ground; however, a major concern is

the extent to which the surf zone whitecaps are representative of whitecaps in the open ocean. The size spectra are very different for bubbles larger than about 50 µm radius, and surf zone bubble number concentrations can be two orders of magnitude larger than those in the open ocean (Brooks et al., 2009a). The wave breaking process in the
5 surf zone results from interaction with the sea bed whereas in the open ocean wave breaking is forced by wind stress and wave-wave interactions. It has not been verified that the aerosol spectra produced are the same in the surf zone, and the open ocean (Lewis and Schwartz, 2004).

Here we present near-surface measurements of aerosol spectra over open ocean
10 whitecaps in the North Atlantic, derive sea spray production fluxes per unit area white-cap, and finally make estimates of the mean surface source fluxes.

2 Measurements

In order to estimate the production of sea spray aerosol from individual wave breaking events a Compact Lightweight Aerosol Spectrometer Probe (CLASP)(Hill et al., 2008)
15 was mounted on a small buoy with an inlet approximately 1 m above the surface (Fig. 1). The buoy was deployed from the *RRS Discovery* during the two cruises of the Sea Spray, Gas Flux, and Whitecaps (SEASAW) project, part of the UK contribution to the international Surface Ocean Lower Atmosphere Study (SOLAS) (Brooks et al., 2009a, b). The cruises were undertaken in the North Atlantic off the west coast of Scotland
20 and Ireland during the periods 7 November to 2 December 2006 (D313) and 21 March to 12 April 2007 (D317). The buoy is surface following but held in a fixed location, ∼ 8 m from the ship, by a weighted cable suspended from a crane. The wire passes through the buoy's tubular central column, allowing the buoy to ride freely up and down the cable as waves pass it. The weight is held at a depth of roughly 25 m below the ocean
25 surface, beneath the immediate effect of wave motions so as to help restrict sideways movement of the buoy. Power and serial communications to CLASP were provided by a single cable running from the ship.

CLASP provides a 16-channel size spectrum at ambient relative humidity covering the size range $0.12 < R_{amb} < 9.25\,\mu m$ at a sample rate of 10 Hz (Hill et al., 2008). The inlet is 0.25 m in length, with one 60 degree bend; particle losses to the walls of the inlet are negligible for particles with radii below 1 µm, 10 % at 3 µm and 20 % at 5 µm. These losses are determined specifically for this inlet and conditions experienced here using the model of Pui et al. (1987) and corrections applied to the spectra. The humidity at 1 m was estimated based on a log profile, using the measured humidity at 21 m and an effective relative humidity at the sea surface of 98 % (Lewis and Schwartz, 2004). Size spectra are subsequently adjusted to 80 % relative humidity via Gerber's (1985) growth model for sea-salt.

A video-based bubble measuring system (Leifer et al., 2003a) was mounted on the underside of the buoy, approximately 0.4 m below the surface to make measurements of bubble size spectra in the range 13–620 µm (radius). The sample volume ($20 \times 2.9 \times 1.9$ mm) is imaged by a video camera, illuminated on-axis from directly opposite the camera. Bubbles appear as a dark ring with a brighter surrounding ring and central bright spot. An automated algorithm identifies candidate bubbles, while rejecting other particles such as algae. Full technical details of system and image processing algorithms are given by Leifer et al. (2003a). The system has previously been used to examine bubble spectra in both the ocean (de Leeuw and Cohen, 2001; de Leeuw et al., 2003, Norris et al., 2011) and the laboratory (Mårtensson et al., 2003 (MN03 hereafter); Leifer et al., 2003b; Sellegri et al., 2006; Fuentes et al., 2010; Hultin et al., 2010; Zabori et al., 2012). Two minutes of image data were collected at five minute intervals throughout each deployment. A total of 154 two-minute samples were obtained over 5 successful deployments: 4 during D317 in the open ocean and 1 during D313 in a fetch limited (∼ 5 km) environment behind the Isle of Arran. Each deployment lasted for between one and four hours.

A vertically oriented accelerometer allowed the movement of the buoy over the waves to be determined, along with estimates of the individual wave heights. One-second resolution digital images of the buoy and the surrounding ocean surface were recorded

from a webcam on the ship providing a visual check on the buoy and the surface conditions in its immediate vicinity. Two Nikon Coolpix 8800 digital SLR cameras were installed on the port side of the bridge, approximately 13 m above sea level, from which to estimate the whitecap fraction of breaking waves at the sea surface (Brooks et al., 2009a, b). Images were taken every 30 s during daylight hours. During analysis a portion of each image was selected which excluded the region where interference by the ship on the wave field was visible, cropped out the sky, and minimised the effects of increased brightness close to the horizon. The automated image processing algorithm of Callaghan and White (2009) was used to determine the whitecap fraction for each image. This determines a suitable threshold intensity value for each image with which whitecaps can be separated from the background water. Although effective, the algorithm can fail under some conditions; as a quality control measure each processed image was manually checked to verify its suitability. Images are rejected if they had contamination from sun-glint, sky reflection, birds within the image, or uneven illumination resulting in misidentification of whitecap area by the automated algorithm. Multiple images were averaged to obtain a total of 63 15-min mean whitecap fractions during the periods for which the buoy was deployed.

Mean meteorological conditions were obtained from meteorology sensors, located on the foremast (see Brooks et al., 2009b for details). 1-dimensional wave spectra and statistics were obtained from a ship borne wave recorder (SBWR) (Tucker and Pitt, 2001; Holliday et al., 2006). The meteorological and oceanographic conditions during the deployments are summarized in Table 1 and Fig. 2.

3 Results

3.1 Mean aerosol concentrations

The source footprint of aerosol reaching the CLASP instrument on the tethered buoy is small, $\sim$ 3 m estimated using the model of Horst and Weil (1992); thus it should be

possible to isolate the spectrum produced by individual whitecaps occurring around the buoy from the mean background spectrum. Figure 3 shows a portion of the time series of total aerosol number concentration from the deployment on 31 March 2007 during cruise D317. Short periods, typically of the order of a few seconds in duration, have particle total number concentrations greater than that for the majority of the record by a factor of 3–7. Comparison of the concentration time series with the photographic record of the buoy shows that these peaks in concentration correspond with the occurrence of whitecaps around the buoy.

A threshold for fresh whitecap aerosol plumes was determined for each individual deployment by applying a 30 point (3-s) running median to the total number concentration time series and accepting concentrations greater than two standard deviations above the median. An absolute threshold of approximately double the mean total concentration, N, for each deployment was also applied in order to fully capture plumes lasting longer than three seconds. The mean whitecap aerosol plume concentration, dN/dR_{80} was an average of 30 % higher than the background concentration.

Aerosol concentrations greater than the threshold level correspond to sampling fresh plumes over whitecaps and are a mixture of aerosol resulting directly from the whitecap with that of the background, while concentrations below the threshold represent the ambient background aerosol spectra. The difference between the two provides an estimate of the mean fresh aerosol concentration generated by the whitecaps, dN/dR_{80}. The variation in the individual whitecap aerosol concentration between the different buoy deployments ranges from less than a factor of two at $R_{80} = \sim 0.25\,\mu m$ up to an order of magnitude for particles with $R_{80} > 2\,\mu m$.

3.2 Bubble concentrations

Figure 4 shows the mean bubble spectra from each deployment. Also shown for comparison are those from the MN03 laboratory study at water temperatures of 5° C and 15° C (measured with the same instrument used here), three open ocean spectra (de Leeuw et al., 2003; Phelps and Leighton, 1998; and measurements from DOGEE

summarised by Brooks et al., 2009a) and two spectra measured in the surf zone (Phelps et al., 1997; Deane and Stokes, 1999). For completion we have also included bubble spectra from three additional buoy deployments (4, 5 April and 28 March) where there were no aerosol data available, but were obtained at wind speeds of 10–11 m s^{-1},

5 lying between those of the other deployments. The mean conditions for these cases are also shown in Table 1. For the smallest bubble sizes the concentrations span just over three orders of magnitude across the SEASAW deployments while for $R > 50$ μm there is much less variability – about one order of magnitude. The observations shown in Fig. 4 are for different wind speeds (5–15 m s^{-1}) and thus large differences in the bub-

10 ble concentrations and spectral distributions would be expected. However, although the wind speed is consistent across 24, 30, 31 March (14.1–14.3 m s^{-1}) there remain significant differences in the bubble spectra; this may result from the variation in wave state and whitecap fraction between these deployments (Table 1). The bubble spectra from the 20 November (15 m s^{-1}) has a number of peaks and the bubble concentration

15 drop off more steeply with increasing bubble size than the other spectra. The ocean conditions were very different on this deployment compared to the three high wind deployments in March 2007 due to the limited fetch of the deployment site, ~ 5 km. The wave heights were very low with a significant wave height of only 0.98 m compared to ~ 3 m for the 14 m s^{-1} deployments. All the other buoy deployments have fetches

20 greater than 500 km for which the wind history is a more important factor than fetch on wave state.

The SEASAW bubble spectra broadly agree with the three other open ocean spectra. All have similar shapes, span a similar range of concentrations and show a similar increase in concentration of the smallest bubbles with increasing wind speed. The

25 surf zone spectra have concentrations 2–3 orders of magnitude higher than the open ocean spectra across the whole measured size range; the difference increasing slightly with increasing size. The MN03 laboratory spectra have concentrations similar to the open ocean spectra for $R < 50$ μm, but increase at larger sizes, and match the surf zone spectra for $100 < R < 350$ μm. The bimodal distribution of the MN03 spectra is not

observed in any of the natural bubble spectra, and is likely due to the artificial method of generation. The variability of individual 2-min estimates of the bubble spectra about the deployment mean is illustrated in Fig. 5 for the cases with one of the highest (31 March, $14\,\mathrm{m\,s^{-1}}$) and lowest (1 April, $7\,\mathrm{m\,s^{-1}}$) wind speeds under open ocean conditions. For bubbles smaller than 300 µm the difference between deployments is much greater than the variability about the deployment mean spectra; for larger bubbles the variability increases significantly – this is due primarily to the occurrence of individual spectral estimates with no bubbles in some of the larger size bins. Note that the bubble spectra measured here are time averages over the whole deployment and are not restricted to freshly generated plumes in breaking waves. However, within the near surface layer (depth < 1 m), bubble populations have been found to be persistent, varying little over time (Farmer and Vagle, 1989). Leifer et al. (2006) showed that the smallest bubbles (< 200 µm) remain in the surface waters after the main body of the plume has surfaced. Bubble terminal rise velocities were calculated following Leifer et al. (2000); they range from $0.0005\,\mathrm{m\,s^{-1}}$ at $R = 15\,\mu\mathrm{m}$ to $0.14\,\mathrm{m\,s^{-1}}$ at $R = 570\,\mu\mathrm{m}$ (the largest mean radius measured). The bubble rise velocities suggest that bubbles smaller than a few hundred µm can be considered well mixed, with only the largest likely to be significantly depleted between wave breaking events.

3.3 Whitecap coverage

It is well understood that the whitecap fraction on the ocean surface increases with wind speed (Monahan and O'Muircheartaigh, 1980). Figure 6 shows the Monahan and O'Muircheartaigh (1980) parameterisation (Eq. 1) along with that of Callaghan et al. (2008) and one derived from the measurements obtained during the SEASAW cruises (following the method of Monahan and Lu, 1990):

$$W = 1.03 \times 10^{-3}(U_{10} - 2.62)^3 \tag{2}$$

The SEASAW whitecap parameterization is very similar to that of Callaghan et al. (2008) in the wind speed range 8 to $17\,\mathrm{m\,s^{-1}}$ but drops off faster at lower wind speeds.

Both are systematically lower than Monahan and O'Muircheartaigh (1980) as are most of the whitecap fractions observed over the last 10 yr (de Leeuw et al., 2011). The 15-min average whitecap estimates for periods matching the bubble spectra estimates during each of deployment are also shown. The overall mean whitecap fractions for each buoy deployment period are given in Table 1. At low wind speeds, 3 to $5\,\mathrm{m\,s}^{-1}$, the whitecap parameterizations become problematic and all three of Monahan and O'Muireartaigh (1980), Callaghan et al. (2008) and the SEASAW parameterisations predict low whitecap fractions at this wind speed though they differ by more than an order of magnitude (Fig. 6).

3.4   Aerosol fluxes

The sea spray source flux, F, is defined here as the product of the particle production flux per unit area of whitecap, F_p, and the % whitecap coverage W:

$$\frac{\mathrm{d}F}{\mathrm{d}R_{80}} = W \times \left(\frac{\mathrm{d}F_p}{\mathrm{d}R_{80}}\right) \qquad (3)$$

First we estimate F_p, the particle production flux per unit area whitecap from the aerosol concentrations. The aerosol concentrations measured on the buoy reflect the net effect of the particle production during the residence time of the air advected past the whitecaps around the buoy. The production flux, F_p, can be estimated as the product of the aerosol number concentration, $\mathrm{d}N/\mathrm{d}R$, with the height of the aerosol plume divided by the residence time of the plume over the whitecap. Precise measurements are not available and so we rely here on characteristic scales. A characteristic plume height can be estimated as the product of a turbulent velocity scale – the friction velocity u_* – and transit time over the whitecap. The particle production flux is thus estimated simply as aerosol number concentration multiplied by u_*.

$$\frac{\mathrm{d}F_p}{\mathrm{d}R_{80}} = \left(\frac{\mathrm{d}N}{\mathrm{d}R_{80}}\right) u_* \qquad (4)$$

Field measurements of aerosol production

S. J. Norris et al.

Title Page

Abstract	Introduction
Conclusions	References
Tables	Figures

|◄   ►|

◄   ►

| Back | Close |

Full Screen / Esc

Printer-friendly Version

Interactive Discussion

The production fluxes for each deployment are shown in Fig. 7, along with production fluxes from MN03, Clarke et al. (2006), and de Leeuw et al. (2000). Conditions for both this and the 3 previous studies are summarised in Table 2. For particles smaller than about 1 µm the SEASAW production fluxes show an increasing trend with wind speed; the majority of them (except 1 April) are a factor of 6–7 higher than those of MN03 and Clarke et al. (2006), but drop off more rapidly with increasing size. For larger particles the production flux is lower than those of the previous studies, and there is no distinct trend with wind speed.

Some factors that may contribute to the differences from earlier studies include water temperature, salinity, and bubble population. MN03 showed that water temperature can have a significant effect on the aerosol spectra produced; increased water temperature resulted in an increase in the number concentration of aerosols with $R_{80} > 0.1$ µm and a decrease for $R_{80} < 0.1$ µm, thus a steeper gradient with size at lower water temperatures. The MN03 production flux for a range of water temperatures from 5 to 25 °C is shown in Fig. 7. The gradient of the SEASAW fluxes for particles larger than 1 µm is steeper than the other functions but for 3 µm particles the SEASAW fluxes are similar to the MN03 flux at 5 °C. The water temperatures during SEASAW varied in a narrow range from 9 °C to 11.2 °C (Table 1). The de Leeuw et al. (2000) study (January 1996 and April 1997, Scripps pier, La Jolla, California) had a water temperature between 13 and 18 °C (NOAA NODC) while climatologically the water temperature at the location and time for that of Clarke et al. (2006) (Hawaii) is ~ 25 °C (NOAA NODC). The warmer waters of the de Leeuw and Clarke campaigns may contribute to the shallower gradient of these two functions compared to the SEASAW fluxes but it is hard to state which out of the many different variables (e.g. water temperature, wind speed, breaking mechanism) is the dominant factor.

The number and size of the bubbles has a strong influence on the aerosol spectrum produced. Both the de Leeuw and Clarke aerosol functions are derived from whitecaps produced in the surf zone where the bubble population is very different to that in the open ocean; while the MN03 function is derived from a laboratory/tank bubble

spectrum that differs from both natural open-ocean and surf zone spectra (Fig. 4). The much higher concentrations of bubbles in these studies compared to the open ocean measurements made here provides a plausible explanation for the higher production fluxes of larger aerosol particles found in the surf zone studies compared to SEASAW and MN03. Jet droplets, between about 1 and 10 µm radius, are produced by the smallest (< 200 µm diameter) bubbles (Blanchard, 1983), where both SEASAW and MN03 have bubble concentrations 1–2 orders of magnitude lower than in the surface zone. It is worth noting that the bubble spectra measured below the ocean surface is not necessarily identical to that from which aerosols are generated at the surface. Small bubbles can merge changing the spectral shape. This makes it difficult to relate the measured bubble spectra directly to the aerosol fluxes.

Sea spray source fluxes were estimated by scaling the production fluxes with the measured whitecap fractions for each deployment (Eq. 3) (Fig. 8); they were also estimated via both the Monahan and O'Muircheartaigh (1980) and the SEASAW whitecap parameterisations. Also shown in Fig. 8 are a number of other sea spray source functions based on whitecap fraction, and one (Norris et al., 2012), that is derived from direct eddy covariance measurements of the aerosol flux made during the same SEASAW cruise (D317) as most of the buoy measurements presented here. All the previous source functions, apart from Norris et al. (2012), use the Monahan and O'Muircheartaigh (1980) whitecap parameterisation in their calculations of the fluxes; differences between them thus result from differences in their specification of the production flux per unit area whitecap. For aerosol in the range $0.1 < R_{80} < 1$ µm, all the source functions, and source flux estimated here for $7\,\mathrm{m\,s^{-1}}$ group within about 1 order of magnitude – this is typical of the spread in the best current estimates (de Leeuw et al., 2011) however for the higher wind speed deployments the spread increases up to nearly 2 orders of magnitude at winds of $15\,\mathrm{m\,s^{-1}}$. The sub-micron in situ flux estimates increase more with wind speed than most of the other source functions, matching them at $7\,\mathrm{m\,s^{-1}}$ on 1st April, sitting a factor of 2–3 above on 30 and 31 March ($14\,\mathrm{m\,s^{-1}}$) and higher than any on 24 March ($14\,\mathrm{m\,s^{-1}}$) and 20 November ($15\,\mathrm{m\,s^{-1}}$). At larger particles sizes

Title Page

Abstract | Introduction

Conclusions | References

Tables | Figures

|◄ | ►|

◄ | ►

Back | Close

Full Screen / Esc

Printer-friendly Version

Interactive Discussion

the source fluxes diverge substantially; the SEASAW estimates being both lowest and decreasing most rapidly with increasing size. There is some indication for dependence of sub-micron in situ flux estimates with wind history. The wind history for each deployment is stated in Table 1. When the wind speed is decreasing slowly (1 April) the in-situ source flux is matches the other source functions, when it is steady (30 and 31 March) they are on the upper edge of the other source functions and when the wind speed is increasing (24 March) and increasing rapidly (20 November) the in-situ source flux is larger than the other source functions by up to an order of magnitude.

Individual eddy covariance (EC) source flux estimates made on the foremast of the ship during the periods of the buoy deployments are also shown in Fig. 8. There is no EC data available for the 20 November. These EC flux estimates are a subset of those used to formulate the Norris et al. (2012) source function. For particles $R_{80} < 1\,\mu m$, both the Norris et al. (2012) function and the individual fluxes from the EC method are up to 1 order of magnitude below the calculated buoy deployment fluxes except for the 1st April. For particles of $R_{80} > 1\,\mu m$ the EC fluxes and the Norris et al. (2012) function are just larger than the buoy flux estimate for the 1 April; they are within the variability of the buoy estimates for the 30 and 31 March deployments; but for the 24 March deployment, all the individual EC measurements are lower than any of the other source fluxes. For the lowest wind speed deployment on the 1 April the individual EC fluxes scatter across the full range of the various source functions. Note that the EC estimates, Norris et al. (2012) and both de Leeuw et al. (2000) and Clarke et al. (2006) are effective fluxes at the measurement height, while all others on figure 8 are interfacial fluxes; however for $R_{80} < 10\,\mu m$ interfacial and effective source fluxes differ little and are often assumed to be directly comparable (de Leeuw et al., 2011).

4 Conclusions

Sea spray source fluxes have been estimated from joint in situ measurements of the aerosol produced by individual whitecaps and the fractional coverage of whitecaps

in the open ocean of the North Atlantic. Near-surface measurements of aerosol size spectra were made at 1 m above the sea surface, from a small tethered buoy, and mean production fluxes estimated for a unit area of whitecap. The mean sea spray source flux was then estimated by scaling the whitecap production flux with the observed whitecap

5   fraction. Sea spray source fluxes were also estimated using two parameterizations of whitecap fraction: Monahan and O'Muircheartaigh, 1980) – the most widely used parameterization – and one that was derived from measurements made during the SEASAW cruises.

The bubble size spectra were measured approximately 0.4 m below the surface from the

10 same buoy as the aerosol. The bubble spectra are comparable to previous measurements in the open ocean, but are 2–3 orders of magnitude lower than measurements in the surf zone. They are also about 2 orders of magnitude lower than the laboratory measurements of Mårtensson et al. (2003) for bubbles larger than about 100 μm. Bubble concentrations increase with wind speed. The limited range of wind speeds en-

15 countered during the buoy deployments precludes developing a full sea spray source function; however the results are instructive.

The aerosol production flux per unit area of whitecap derived from mean particle spectra was found to vary with wind speed: for particles with R_{80} below approximately 1–2 μm the production flux increased with wind speed, while for larger particles there

20 was no clear dependence, but concentration decreased more rapidly with size than do the production flux spectra of the earlier studies. This behaviour is consistent with the observed overall increase in bubble concentrations with wind speed, and implies that a simple single aerosol production flux cannot be defined and scaled by whitecap fraction to determine the mean sea spray source flux. We note however, that the previous

25 source functions adopting this approach do generally define a single production flux, often from relatively limited ranges of forcing conditions and unrepresentative of open ocean conditions. Clarke et al. (2006) used measurements at only a single wind speed. de Leeuw et al. (2000) do defined a wind-speed dependent function valid for winds up

to $9\,\mathrm{m\,s^{-1}}$, but since the measurements are from the surf zone, the physics of the wave breaking is rather different from that in the open ocean.

The differences between the observed production flux spectra on each day may be a direct result of the differences in bubble spectra, and to a more limited extent water properties, for each deployment. In situ whitecap fraction estimates corresponding to each bubble measurement period were very scattered, but in general agreed with a parameterization derived from the full set of whitecap imagery obtained during SEA-SAW, and with that of Callaghan et al. (2008); all of these are significantly lower than the widely used parameterization of Monahan and O'Muircheartaigh (1980).

The mean source flux estimates reflect the production flux results: for $R_{80} < 1\,\mu\mathrm{m}$ the flux spectra span the values from previous studies (Monahan, 1986; de Leeuw et al., 2000; Mårtensson et al., 2003; Clarke et al., 2006), but decrease more rapidly with increasing size for larger particles. The mean source flux estimates and the EC flux derived source function of Norris et al. (2012) all decrease more rapidly with increasing particle size than the surf zone functions. This is consistent with the much higher bubble concentrations observed in surf zone spectra compared with the open ocean spectra. This confirms the suggestion (Lewis and Schwartz, 2004) that the surf zone is not representative of open ocean bubble populations and aerosol production, since the bubble production is modified through the wave interaction with the shelving beach.

References

Andreas, E. L.: A review of the sea spray generation function for the open ocean, in: Atmosphere-Ocean Interactions, Vol. 1, edited by: Perrie, W., 1–46, WIT Press, Southampton, UK, 2002.

Andreas, E. L, Jones, K. F., and Fairall, C. W.: Production velocity of sea spray droplets, J. Geophys. Res., 115, C12065, doi:10.1029/2010JC006458, 2010.

Anguelova, M. D. and Webster, F.: Whitecap coverage from satellite measurements: A first step toward modelling the variability of oceanic whitecaps, J. Geophys. Res., 111, C03017, doi:10.1029/2005JC003158, 2006.

Blanchard, D. C.: The electrification of the atmosphere by particles from bubbles in the sea, Program of Oceanography, 1, 171–202, 1963.

Blanchard, D. C.: The oceanic production rate of cloud nuclei, J. Recherches Atmos., 4, 1–6, 1969.

Blanchard, D. C.: The Production, Distribution, and Bacterial Enrichment of the Sea-Salt Aerosol, in: Air-Sea Exchange of Gases and Particles, edited by: Slinn, W. G. N. and Liss, P. S., Kluwer Academic Publishers, 1983.

Blanchard, D. C.: Surface-active monolayers, bubbles and jet drops, Tellus, 42B, 200–205, 1990.

Blanchard, D. C. and Woodcock, A.: Bubble formation and modification in the sea and its meteorological significance, Tellus, 9, 145–158, 1957.

Bortkovskii, R. S.: Air-sea exchange of heat and moisture during storms, Springer, New York, 193 pp., 1987.

Brooks, I. M., Yelland, M. J., Upstill-Goddard, R. C., Nightingale, P. D., Archer, S., d'Asaro, E., Beale, R., Beatty, C., Blomquist, B., Bloom, A. A., Brooks, B. J., Cluderay, J., Coles, D., Dacey, J., DeGrandpre, M., Dixon, J., Drennan, W. M., Gabriele, J., Goldson, L., Hardman-Mountford, N., Hill, M. K., Horn, M., Hsueh, P. - C., Huebert, B., de Leeuw, G., Leighton, T. G., Liddicoat, M., Lingard, J. J. N., McNeil, C., McQuaid, J. B., Moat, B. I., Moore, G., Neill, C., Norris, S. J., O'Doherty, S., Pascal, R. W., Prytherch, J., Rebozo, M., Sahlee, E., Salter, M., Schuster, U., Skjelvan, I., Slagter, H., Smith, M. H., Smith, P. D., Srokosz, M., Stephens, J. A., Taylor, P. K., Telszewski, M., Walsh, R., Ward, B., Woolf, D. K., Young, D., and Zemmelink, H.: Physical Exchanges at the Air-Sea, Interface: Field Measurements from UK-SOLAS, Bull. Amer. Meteorol. Soc., 90, 629–644, doi:10.1175/2008BAMS2578.1, 2009a.

Brooks, I. M., Yelland, M. J., Upstill-Goddard, R. C., Nightingale, P. D., Archer, S., d'Asaro, E., Beale, R., Beatty, C., Blomquist, B., Bloom, A. A., Brooks, B. J., Cluderay, J., Coles, D., Dacey, J., DeGrandpre, M., Dixon, J., Drennan, W. M., Gabriele, J., Goldson, L., Hardman-Mountford, N., Hill, M. K., Horn, M., Hsueh, P.-C., Huebert, B., de Leeuw, G., Leighton, T. G., Liddicoat, M., Lingard, J. J. N., McNeil, C., McQuaid, J. B., Moat, B. I., Moore, G., Neill, C., Norris, S. J., O'Doherty, S., Pascal, R. W., Prytherch, J., Rebozo, M., Sahlee, E., Salter, M., Schuster, U., Skjelvan, I., Slagter, H., Smith, M. H., Smith, P. D., Srokosz, M., Stephens, J. A., Taylor, P. K., Telszewski, M., Walsh, R., Ward, B., Woolf, D. K., Young, D., and Zemmelink, H.: UK-SOLAS Field Measurements of Air-Sea, Exchange: Instrumentation, Bull. Amer. Meteorol. Soc., 90 (electronic supplement), 9–16, doi:10.1175/2008BAMS2578.2, 2009b.

Callaghan, A. H. and White, M.: Automated processing of sea surface images for the determination of whitecap coverage, J. Atmos. Ocean. Tech., 26, 383–394, 2009.

Callaghan, A. H., de Leeuw, G., Cohen, L., and O'Dowd, C. D.: Relationship of oceanic whitecap coverage to wind speed and wind history, Geophys. Res. Lett., 35, L23609, doi:10.1029/2008GL036165, 2008.

Cipriano, R. J., Blanchard, D. C., Hogan, A. W., and Lala, G. G.: On the production of Aitken nuclei from breaking waves and their role in the atmosphere, J. Atmos. Sci., 40, 469–479, 1983.

Cipriano, R. J., Monahan, E. C., Bowyer, P. A., and Woolf, D. K.: Marine condensation nucleus generation inferred from whitecap simulation tank results, J. Geophys. Res., 92, 6569–6576, 1987.

Clarke, A. D., Owens, S. R., and Zhou, J.: An ultra fine sea-salt flux from breaking wave: Implications for cloud condensation nuclei in the remote marine atmosphere, J. Geophys. Res., 111, D06202, doi:10.1029/2005JD006565, 2006.

Day, J. A.: Production of droplets and salt nuclei by the bursting of air bubble films, Quart. J. Roy. Meteor. Soc., 90, 72–78, 1964.

Deane, G. B. and Stokes, M. D.: Air entrainment processes and bubble size distributions in the surf zone, J. Phys. Oceanogr., 29, 1393–1403, 1999.

de Leeuw, G.: The occurrence of large salt-water droplets at low-elevations over the open ocean, in: The Climate and Health Implications of Bubble-Mediated Air-Sea Exchange, edited by: Monahan, E. C. and Van Patten, M. A., 65–82, Connecticut Sea Grant College Program CT-SG-89-06, 1989.

de Leeuw, G. and Cohen, L. H.: Bubble size distributions on the North Atlantic and the North Sea in Gas Transfer and water Surfaces, edited by: Donelan, M. A., Drennan, W. M., Salzman, E. S., and Wanninkhof, R., 271–277, AGU, 2001.

de Leeuw, G., Neele, F. P., Hill, M., Smith, M. H., and Vignati, E.: Production of sea spray aerosol in the surf zone, J. Geophys. Res., 105, 29397–29409, 2000.

de Leeuw, G., Moerman, M., Cohen, L., Brooks, B., Smith, M., and Vignati, E.: Aerosols, bubbles and sea spray production studies during the RED experiments, Proceedings AMS conference, Long Beach, CA, 9–13 February, 2003.

de Leeuw, G., Andreas, E. L., Anguelova, M. D., Fairall, C. W., Lewis, E. R., O'Dowd, C., Schulz, M., and Schwartz, S. E.: Production Flux of Sea-Spray Aerosol, Rev. Geophys., 49, RG2001, doi:10.1029/2010RG000349, 2011.

Facchini, M. C., Rinaldi, M., Decesari, S., Carbone, C., Finessi, E., Mircea, M., Fuzzi, S., Ceburnis, D., Flannigan, R., Nilsson, E. D., de Leeuw, G., Martino, M., Woeltjen, J., and O'Dowd, C. D.: Primary submicron marine aerosol dominated by insoluble organic colloids and aggregates, Geophys. Res. Lett., 35, L17814, doi:10.1029/2008GL034210, 2008.

Farmer, D. M. and Vagil, S.: Waveguide propagation of ambient sound in the ocean-surface bubble layer, J. Acoust. Soc. Am., 86, 1897–1908, 1989.

Fuentes, E., Coe, H., Green, D., de Leeuw, G., and McFiggans, G.: Laboratory-generated primary marine aerosol via bubble-bursting and atomization, Atmos. Meas. Tech., 3, 141–162, doi:10.5194/amt-3-141-2010, 2010.

Georgescu, S.-C., Achard, J., and Canot, E.: Jet drops ejection in bursting gas bubble processes, European Journal of Mechanics B/Fluids, 21, 265–280, 2002.

Gerber, H. E.: Relative-humidity parameterization of the navy aerosol model (NAM), Report No. NRL Report 8956, 17, Navel Research Laboratory, Washington, DC, 1985.

Haywood, J. M., Ramaswamy, V., and Soden, B. J.: Tropospheric Aerosol Climate Forcing in Clear-Sky Satellite Observations over the Ocean, Science, 283, 1299–1303, 1999.

Hill, M. K., Brooks, B. J., Norris, S. J., Smith, M. H., Brooks, I. M., de Leeuw, G., and Lingard, J. J. N.: A Compact Lightweight Aerosol Spectrometer Probe (CLASP), J. Atmos. Oceanic. Technol., 25, 1996–2006, doi:10.1175/2008JTECHA1051.1, 2008.

Holliday, N. P., Yelland, M. J., Pascal, R. W., Swail, V. R., Taylor, P. K., Griffiths, C. R., and Kent, E. C.: Were extreme waves in the Rockall Trough the largest ever recorded?, Geophys. Res. Lett., 33, L05613, doi:10.1029/2005GL025238, 2006.

Title Page

Abstract | Introduction

Conclusions | References

Tables | Figures

◄ | ►

Back | Close

Full Screen / Esc

Printer-friendly Version

Interactive Discussion

Hoppel, W. A., Frick, G. M., and Fitzgerald, J. W.: The Surface Source Function for Sea-Salt Aerosol and Aerosol Dry Deposition to the Ocean Surface, J. Geophys. Res., 107, 4382–4399, 2002.

Horst, T. W. and Weil, J. C.: Footprint Estimation for Scalar Flux Measurements in the Atmospheric Surface Layer, Bound.-Layer Meteorol., 59, 279–296, 1992.

Hultin, K. A. H., Nilsson, E. D., Krejci, R., Mårtensson, E. M., Ehn, M., Hagström, Å., and de Leeuw, G.: In situ laboratory sea spray production during the Marine Aerosol Production 2006 cruise on the northeastern Atlantic Ocean, J. Geophys. Res., 115, D06201, doi:10.1029/2009JD012522, 2010.

Johnson, B. D. and Wangersky, P. J.: Microbubbles: Stabilization by monolayers of adsorbed particles, J. Geophys. Res., 92, 14641–14647, 1987.

Keene, W. C., Maring, H., Maben, J. R., Kieber, D. J., Pszenny, A. A. P., Dahl, E. E., Izaguirre, M. A., Davis, A. J., Long, M. S., Zhou, X., Smoydzin, L., and Sander, R.: Chemical and physical characteristics of nascent aerosols produced by bursting bubbles at a model air sea interface, J. Geophys. Res., 112, D21202, doi:10.1029/2007JD008464, 2007.

Kolovayev, P. A.: Investigation of the concentration and statistical size distribution of wind-produced bubbles in the near-surface ocean layer, Oceanology, 15, 659–661, 1976.

Leifer, I., Patro, R. K., and Bowyer, P.: A study on the temperature variation of rise velocity for large clean bubbles. J. Atmos. Oceanic. Technol., 17, 1392–1402, 2000.

Leifer, I., de Leeuw, G., and Cohen, L. H.: Optical Measurement of Bubbles: System Design and Application, J. Atmos. Oceanic. Technol., 20, 1317–1332, 2003a.

Leifer, I., De Leeuw, G., Kunz G., and Cohen, L. H.. Calibrating optical bubble size by the displaced mass method, Chem. Eng. Sci., 58, 5211–5216, 2003b.

Leifer, I., Caulliez, G., and de Leeuw, G.: Bubbles generated from wind-steepened breaking waves: 2. Bubble plumes, bubbles, and wave characteristics, J. Geophys. Res., 111, C06021, doi:101029/2004JC002676, 2006.

Leighton, T. G. and Robb, G. B. N.: Preliminary mapping of void fractions and sound speeds in gassy marine sediments from subbottom profiles, J. Acoust. Soc. Am., 124, EL313–EL320, 2008.

Lewis, E. R. and Schwartz, S. E.: Sea Salt Aerosol Production – Mechanisms, Methods, Measurements, and Models, American Geophysical Union, 2004.

Field measurements of aerosol production

S. J. Norris et al.

Title Page	
Abstract	Introduction
Conclusions	References
Tables	Figures

◄◄	►►
◄	►
Back	Close

Full Screen / Esc

Printer-friendly Version

Interactive Discussion

Mårtensson, E. M., Nilsson, E. D., de Leeuw, G., Cohen, L. H., and Hansson, H. C.: Laboratory simulations and parameterization of the primary marine aerosol production, J. Geophys. Res., 108, 4297, doi:10.1029/2002JD002263, 2003.

Medwin, H.: In situ acoustic measurements of bubble populations in coastal waters, J. Geophys. Res., 75, 599–611, 1970.

Monahan, E. C.: Sea Spray as a function of low elevation wind speed, J. Geophys. Res., 73, 1127–1137, 1968.

Monahan, E. C.: Oceanic whitecaps, J. Phys. Oceanogr., 1, 139–144, 1971.

Monahan, E. C. and Lu, M.: Acoustically relevant bubble assemblages and their dependence on meteorological parameters, IEEE J. Oceanic Engineering, 15, 340–349, 1990.

Monahan, E. C. and O'Muircheartaigh, I.: Optimal Power-Law Description of Oceanic Whitecap Coverage Dependence on Wind Speed, J. Phys. Oceanogr., 10, 2094–2099, 1980.

Monahan, E. C. and O'Muircheartaigh, I.: Review Article: Whitecaps and the Passive Remote Sensing of the Ocean Surface, Int. J. Remote Sens., 7, 627–642, 1986.

Monahan, E. C., Spiel, D. E., and Davidson, K. L.: Whitecap aerosol productivity deduced from simulation tank measurements, J. Geophys. Res., 87, 8898–8904, 1982.

Monahan, E. C., Spiel, D. E., and Davidson, K. L.: A model of marine aerosol generation via whitecaps and wave disruption, in: Oceanic Whitecaps, edited by: Monahan, E. C., and Mac Niocaill, G., D. Reidel Publishing Company, 167–174, 1986.

Morelli, J., Buat-Menard, P., and Chesselet, R.: Production experimentale d'aerosols a la surface de la mer, J. Recherches Atmos., 8, 961–986, 1974.

Norris, S. J., Brooks, I. M., de Leeuw, G., Sirevaag, A., Leck, C., Brooks, B. J., Birch, C. E., and Tjernström, M.: Measurements of bubble size spectra within leads in the Arctic summer pack ice, Ocean Sci., 7, 129–139, doi:10.5194/os-7-129-2011, 2011.

Norris, S. J., Brooks, I. M., Hill, M. K., Brooks, B. J., Smith, M. H., and Sproson, D. A. J.: Eddy Covariance Measurements of the Sea Spray Aerosol Flux over the Open Ocean, J. Geophys. Res., 117, D07210, doi:10.1029/2011JD016549, 2012.

O'Dowd, C. D., Lowe, J. A., and Smith, M. H.: Coupling of sea-salt and sulphate interactions and its impact on cloud droplet concentration predictions, Geophys. Res. Lett., 26, 1311–1314, 1999.

O'Dowd, C. D., Lowe, J. A., Clegg, N., Smith, M. H., and Clegg, S. L.: Modelling heterogeneous sulphate production in maritime straiform clouds, J. Geophys. Res., 105, 7143–7160, 2000.

Field measurements of aerosol production

S. J. Norris et al.

Pascal, R. W., Yelland, M. J., Srokosz, M. A., Moat, B. I., Waugh, E. M., Comben, D. H., Clansdale, A. G., Hartman, M. C., Coles, D. G. H., Hsueh, P. C., and Leighton, T. G.: A spar buoy for high frequency wave measurements and detection of wave breaking in the open ocean, J. Atmos. Oceanic Tech., 28, 590–605, 2011.

5   Parameswaran, K.: Influence of micrometeorological features on coastal boundary layer aerosol characteristics at the tropical station, Trivandrum, Proc. Indian Acad. Sci. (Earth Planet. Sci.), 110, 247–265, 2001.

Phelps, A. D. and Leighton, T. G.: Oceanic bubble population measurements using a buoy-deployed combination frequency technique, IEEE J. Oceanic Eng., 23, 400–410, 1998.

10 Phelps, A. D., Ramble, D. G., and Leighton, T. G.: The use of a combination frequency technique to measure the surf zone bubble population, J. Acoust. Soc. Amer., 101, 1981–1989, 1997.

Pui, D. Y. H., Romay-Novas, F., and Lui, B. Y. H.: Experimental study of particle deposition in bends of circular cross section, Aerosol Sci. Technol., 7, 301–315, 1987.

Sellegri, K., O'Dowd, C. D., Yoon, Y. J., Jennings, S. G., and de Leeuw, G.: Surfactants and sub-

15 micron sea spray generation, J. Geophys. Res., 111, D22215, doi:10.1029/2005JD006658, 2006.

Spiel, D. E.: A study of aerosols generated in a whitecap simulation tank, BDM Tech, Rep. 006-83, Monterey, 35, 1983.

Spiel, D. E.: The sizes of the jet drops produced by air bubbles bursting on sea and fresh-water

20 surfaces, Tellus, 46B, 325–338, 1994.

Spiel, D. E.: A hypothesis concerning the peak in film drop production as a function of bubble size, J. Geophys. Res., 102, 1153–1161, 1997.

Tucker, M. J. and Pitt, E. G.: Waves in Ocean Engineering, Ocean Eng. Book Ser., Vol. 5, Elsevier, New York, 521, 2001.

25 Tyree, C. A., Hellion, V. M., Alexandrova, O. A., and Allen, J. O., Foam droplets generated from natural and artificial seawaters, J. Geophys. Res., 112, D12204, doi:10.1029/2006JD007729, 2007.

Wettlaufer, G.: Introduction to crystallization phenomena in natural and artificial sea ice, in: The Physics of ice covered seas, edited by: Lepparantä, M., Univ. of Helsinki, Helsinki, 105–195,

30 1998.

Woodcock, A. H., Blanchard, D. C., and Rooth, C. G. H.: Salt-induced convection and clouds, J. Atmos. Sci., 20 159–169, 1963.

Field measurements of aerosol production

S. J. Norris et al.

Title Page

Abstract	Introduction
Conclusions	References
Tables	Figures

◄◄   ►►

◄   ►

Back   Close

Full Screen / Esc

Printer-friendly Version

Interactive Discussion

Woolf, D. K., Monahan, E. C., and Spiel, D. E.: Quantification of the marine aerosol produced by whitecaps, in Seventh Congress on Ocean – Atmosphere Interaction, 182–185, American Meteorological Society, Anaheim, CA, 1988.

Wu, J., Murray, J. J., and Lai, R. J.: Production and distributions of sea spray, J. Geophys. Res., 89, 8163–8169, 1984.

Zábori, J., Krejci, R., Ekman, A. M. L., Mårtensson, E. M., Ström, J., de Leeuw, G., and Nilsson, E. D.: Wintertime Arctic Ocean sea water properties and primary marine aerosol concentrations, Atmos. Chem. Phys. Discuss., 12, 16085–16130, doi:10.5194/acpd-12-16085-2012, 2012.

Table 1. Summary of the meteorological and oceanographic conditions including the 10 m wind speed, U_{10}; friction velocity, u_*; air temperature at 21 m, T_a; relative humidity at 1 m and 21 m; water temperature, T_w; salinity, S; mean wave slope, MWS; significant wave height, H_s; and whitecap fraction, W. The entries in italics are for buoy deployments where bubble spectra were obtained but no aerosol data are available.

Date	Times	Cruise	U_{10} (m s^{-1})	u_* (m s^{-1})	T_a (°C) 21 m	RH (%) at 1 m	RH (%) at 21 m	T_w (°C)	S (‰)	MWS	H_s (m)	W (%)
20/11/06 JD 324	11:20–13:15	D313	15.1 rising fast	0.69	8.9	92	67.2	11.2	–	0.01	0.98	2.1258
24/03/07 JD 83	09:15–13:15	D317	14.3 rising slowly	0.51	7.6	92	66.4	9.11	35.5	0.031	3.6	1.9163
28/03/07 JD 87	*09:27–11:20*	*D317*	*10.7 steady*	*0.40*	*6.0*	*91*	*63.4*	*9.32*	*35.2*	*0.032*	*2.2*	*2.11*
30/03/07 JD 89	09:00–10:10	D317	14.2 steady	0.50	8.4	95	86.9	9.04	35.5	0.031	3.3	1.143
31/03/07 JD 90	09:17–11:20	D317	14.1 steady	0.49	8.8	97.5	93.2	9.24	35.5	0.035	2.8	1.48
01/04/07 JD 91	09:05–13:30	D317	7.3 falling slowly	0.24	9.3	97.5	93.4	9.39	36.0	0.031	2.8	0.066
04/04/07 JD 94	*13:20–16:30*	*D317*	*10.7 rising*	*0.41*	*11.4*	*94*	*77.8*	*12.3*	*35.5*	*0.028*	*1.8*	*0.45*
05/04/07 JD 95	*09:10–11:41*	*D317*	*11.3 steady*	*0.43*	*11.9*	*95*	*84.5*	*11.6*	*35.5*	*0.032*	*2.4*	*0.49*

Table 2. Summary of the main studies discussed in this paper. Mårtensson et al. (2003), Clarke et al. (2006) and De Leeuw et al. (2000) all use the Monahan and O'Muircheartaigh (1980) whitecap function.

Study	Method	Water T °C	U_{10} m s^{-1}
Mårtensson et al. (2003)	Tank	5 to 25	–
Clarke et al. (2006)	Surf Zone	~ 25	7.3 ± 1.1
De Leeuw et al. (2000)	Surf Zone	13 to 18	0 to 9
This study	Open Ocean	9 to 11.2	7 to 15
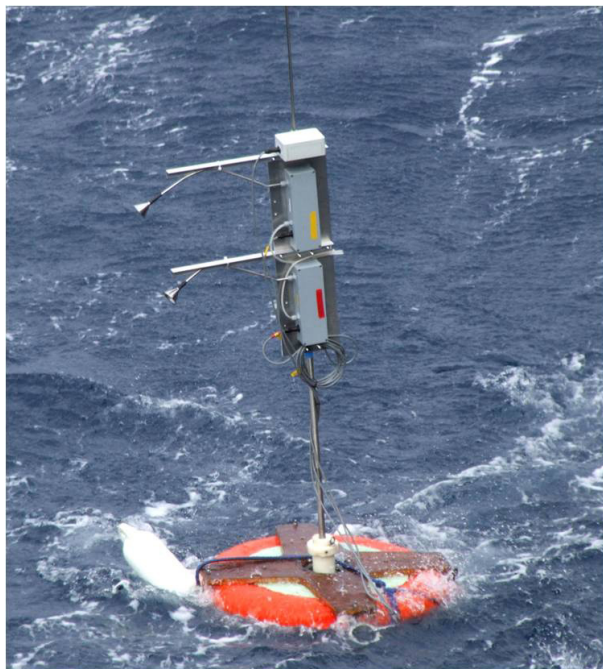
Fig. 1. The tethered-buoy. The inlets to two CLASP units are visible. The lower unit was damaged and not used in subsequent deployments. The bubble imaging system is mounted below the buoy's floatation ring.
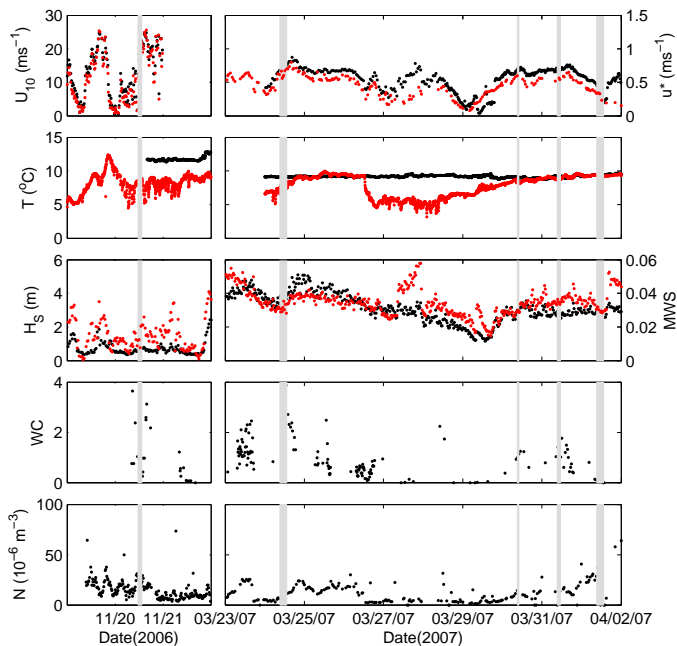
Fig. 2. Time series of mean conditions during the two cruises, the grey shading indicates the duration of the buoy deployments. **(a)** 10 m wind speed, U_{10} m s^{-1} (black) and friction velocity, u_* (m s^{-1}) (red); **(b)** temperature of the air at $\sim$ 17 m (red) and near surface water (black); **(c)** significant wave height H_s (m)(black) and mean wave slope (MWS) (red) calculated from mean wave periods and significant wave height: slopes greater than 0.03 indicate undeveloped sea state, those less than 0.03 indicate a well-developed sea (Bourassa et al., 2001); **(d)** mean half hourly whitecap coverage WC (%); **(e)** CLASP 28 min averages of total particle number concentration (m^{-3}).
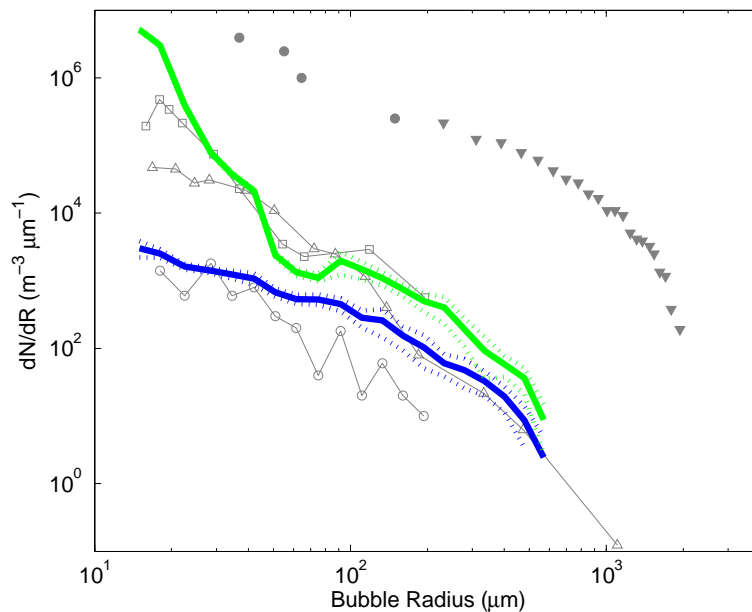
Title Page

Abstract | Introduction

Conclusions | References

Tables | Figures

|◄ | ►|

◄ | ►

Back | Close

Full Screen / Esc

Printer-friendly Version

Interactive Discussion
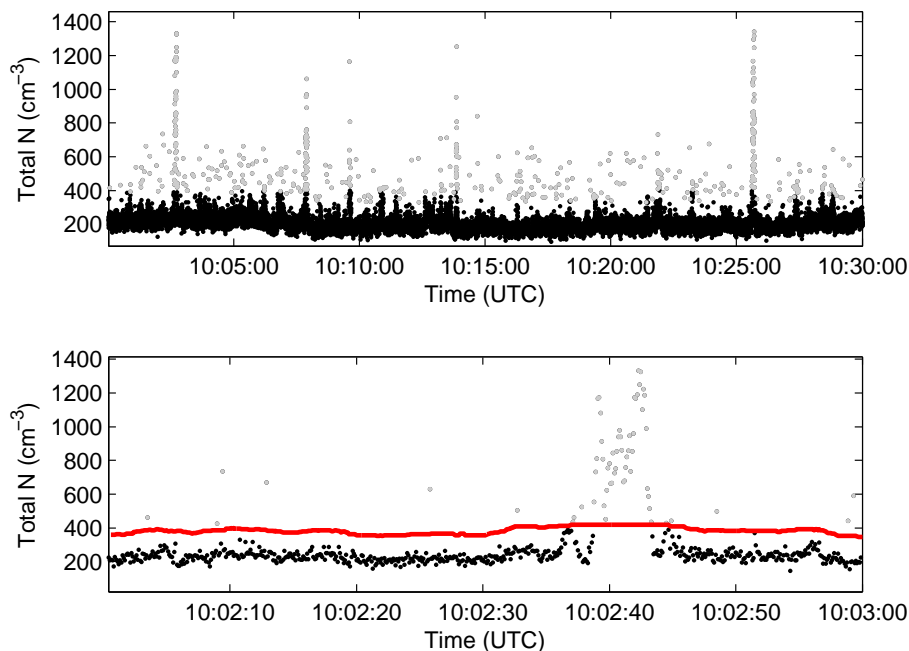
Fig. 3. A 30 min section of the total aerosol number concentration (cm^{-3}) time series (top) and a closer view of 1 min of data (bottom) from the deployment on the 31 March. Grey points are the selected whitecap plumes, black points show the ambient background concentration. The red line depicts the threshold.

Field measurements of aerosol production

S. J. Norris et al.
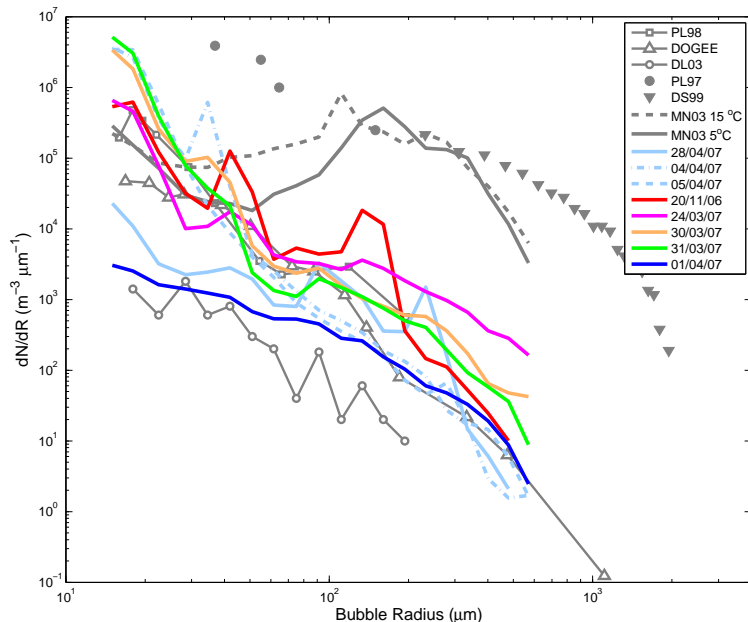
Fig. 4. Mean bubble spectra for each buoy deployment (coloured lines, pale blue lines are cases where no corresponding aerosol measurements are available). A number of previous measurements are shown for comparison (grey lines). The open ocean spectra (open symbols) of de Leeuw et al. (2003) (DL03, $U = 5\,\mathrm{m\,s^{-1}}$), Phelps and Leighton (1998) (PL98, depth 0.5 m, $U = 12$–$14\,\mathrm{m\,s^{-1}}$), and measurements by Leighton and Coles, summarized in Brooks et al. (2009) and Pascal et al. (2011) (DOGEE, averaged over a depth of 0–3 m, $U = 13\,\mathrm{m\,s^{-1}}$), and the surf zone spectra (filled symbols) of Phelps et al. (1997) (P97), and Deane and Stokes (1999) (DS99) along with the laboratory bubbles spectra of Mårtensson et al. (2003) at 5 °C (solid grey line) and 15 °C (dashed grey line) are shown for comparison. The Deane and Stokes (1999) measurements are restricted to actively breaking regions of surf.

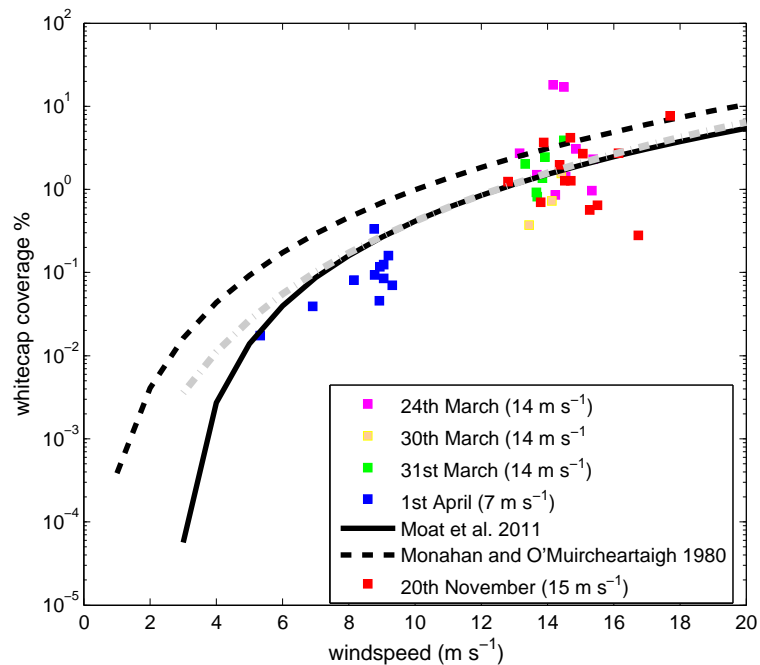**Fig. 5.** The mean bubble size spectra (solid lines) for 1 April (7 m s^{-1} winds, blue) and 31 March (14 m s^{-1} winds, green) and their standard errors (dotted). Open ocean and surf zone spectra in grey are as in Fig. 4.
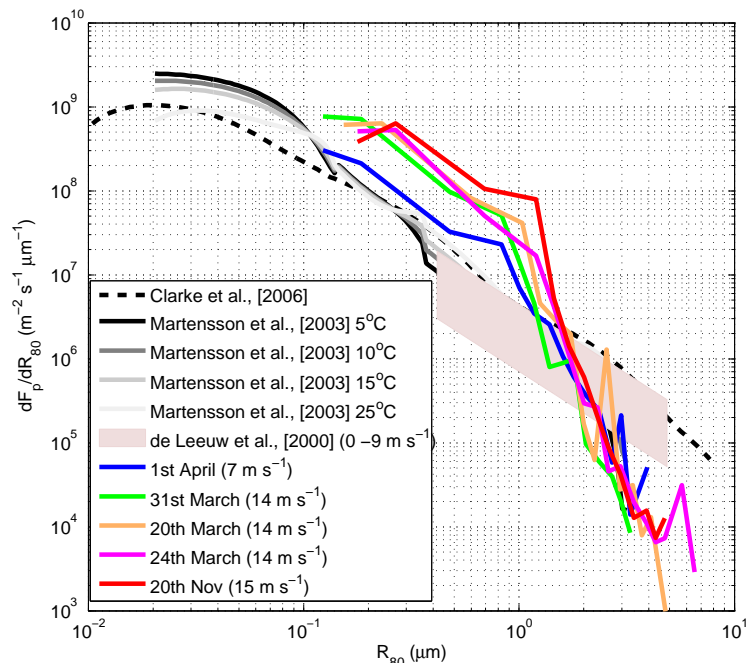
Fig. 6. The SEASAW whitecap estimates during each buoy deployment (symbols), and the whitecap parameterizations from the full SEASAW cruise data set, Callaghan et al. (2008) and Monahan and O'Muireartaigh (1980).

Title Page

Abstract | Introduction

Conclusions | References

Tables | Figures

◄ | ►►|

◄ | ►

Back | Close

Full Screen / Esc

Printer-friendly Version

Interactive Discussion

Fig. 7. The mean production flux per unit area of whitecap for each deployment. The production flux functions from previous studies utilizing similar methods are also shown for comparison. The pink shaded area shows the range of the production fluxes estimated by de Leeuw et al. (2000) for a range of wind speeds between 0 and $9 \, \mathrm{m \, s^{-1}}$. The error estimate for the estimated production flux is the same for all the SEASAW deployments; 38.5 %.
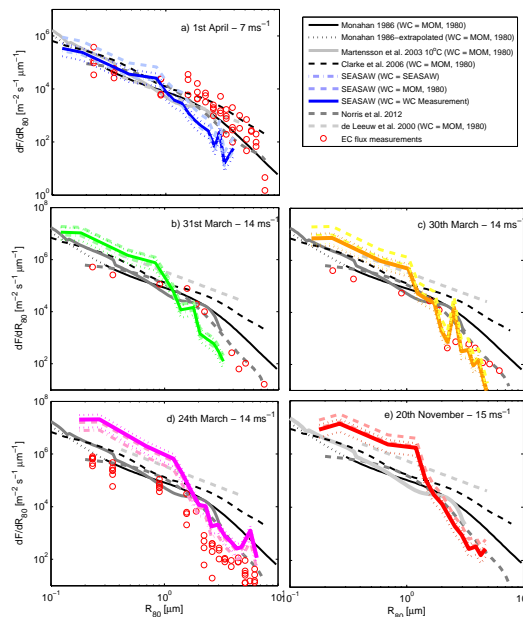
Fig. 8. Mean source fluxes using the production flux estimates (coloured lines) and the measured whitecap fraction (solid lines), and whitecap parameterizations from Monahan and O'Muircheartaigh (1980) (dashed lines) and derived from SEASAW data (dot-dashed lines). The line colours correspond to those used in figures 4–7 to identifying the deployment date. The dotted lines show the uncertainty around the source flux using the measured whitecap coverage. All other source functions (black and grey lines) use the Monahan and O'Muircheartaigh (1980) (MOM, 1980) whitecap parameterisation. The individual 28-min average eddy covariance aerosol flux measurements made during each of the five deployments are plotted as red circles. Please note the y-axis scale on **(a)** is shifted relative to the other panels. Please note the de Leeuw et al. (2000) production flux used is defined at $9\,\mathrm{m\,s^{-1}}$, the maximum wind speed in their study (see Table 2) but is applied here up to $15\,\mathrm{m\,s^{-1}}$.